Geomechanics and Engineering, *Vol. 34, No. 3 (2023) 317-328*
https://doi.org/10.12989/gae.2023.34.3.317

Modelling the critical state behaviour of granular soils: Application of NorSand constitutive law to TP-Lisbon sand

António Viana da Fonseca[a], Fausto Molina-Gómez*, Cristiana Ferreira[b] and Julieth Quintero[c]

CONSTRUCT-GEO, Faculty of Engineering (FEUP), Universidade do Porto, Rua Dr. Roberto Frias, s/n 4200-465 Porto, Portugal

(*Received August 2, 2022, Revised June 20, 2023, Accepted July 6, 2023*)

Abstract. The soil behaviour can be represented by numerical modelling of element testing using diverse constitutive models. However, not all constitutive models allow the simulation of the stress-strain response at the critical state in granular soils with both contractive and dilative behaviour. Moreover, the accuracy of these models depends highly on the quality of the experimental data used for their calibration. This study addresses the modelling of the critical state behaviour of an alluvial natural soil from the Lower Tagus Valley (south of Portugal), known as TP-Lisbon sand, using the NorSand constitutive law. For this purpose, a series of numerical simulations of element testing was carried out using two algorithms performed in Visual Basic (VB) and Fast Lagrangian Analysis of Continua (FLAC). Moreover, this study presents the characterisation of of NorSand parameters from an accurate experimental programme based on triaxial and bender element testing. This experimental program allowed defining: (i) the critical state locus, (ii) the stress-dilatancy, and (iii) the soil elasticity of TP-Lisbon sand —all fundamental to calibrate the contractive and dilative behaviour of such alluvial soil. The results revealed a good agreement between experimental data and NorSand simulations using VB and FLAC. Therefore, this study showed that the quality of laboratory testing procedures and its good interpretation enables NorSand constitutive law to capture representatively the non-associated plastic strains, often expressed by the state parameter, allowing a representation of soil behaviour of alluvial soils within the critical state soil mechanics framework for different state parameters.

Keywords: critical state soil mechanics; numerical modelling; laboratory tests; sands

1. Introduction

Soils are heterogeneous materials formed by natural grains, inducing rheological features that distinguish these materials from other solid materials. Soil behaviour strongly depends on the normal and shear stresses. Both types of stresses generate volumetric or pore-pressure variations, which leads to non-associated plastic strains, often represented by soil dilatancy. Models are useful tools for representing reality (Wood 2004); constitutive models provide mathematical representations of soil behaviour. However, numerous constitutive models assume the soils as a perfectly elastic material (Schofield and Wroth 1968). The validation of numerical models usually comprises experimental data obtained from element tests or physical models (Ramos *et al*. 2015, Molina-Gómez *et al*. 2019).

Advanced constitutive models are designed especially for specific soil types and loading conditions. Because of that, it is common to find models that can only describe the soil behaviour for specific conditions or situations (Won *et al.* 2020). However, the formulation of constitutive models alone is insufficient for solving practical engineering problems. Hence, such models must be implemented in finite or discrete element codes.

Worldwide, a variety of models have been devised to describe soil behaviour. The most widely used constitutive models are elastoplastic models or models based on theories of elasticity, plasticity, viscoplasticity, micro-fracturing and damage mechanics either combined or separately (Desai, 2005, Mendoza and Muniz de Farias 2020, Nieto-Leal and Kaliakin 2021). Conversely, most traditional constitutive models, such as the Mohr-Coulomb model, do not consider the soil response after peak strength, i.e. the critical state condition. Hence, several novel constitutive models have been formulated in the last few decades to assess the monotonic and cyclic behaviour of sands, such as PDMY02 (Yang *et al.* 2003), PM4sand (Boulanger and Ziotopoulou 2017), SANISAND (Taiebat *et al.* 2008), SANISAND-F (Petalas *et al.* 2020) and NorSand (Jefferies 1993). These models can be applied in granular soils since they involve an associated flow rule (i.e., a vector of plastic strain increment normal to the yield surface), using the elements of the Critical State Soil Mechanics (CSSM) framework.

However, the application of these models comprises many parameters, which often require advanced soil testing for their characterisation (Wichtmann *et al.* 2019). Moreover, the performance of advanced models is assessed by numerical modelling of element tests (Wichtmann *et al.* 2019). The validation through element test modelling ensures the correct application of the constitutive models

*Corresponding author, Ph.D. Student
E-mail: fausto@fe.up.pt
[a]Professor
[b]Ph.D.
[c]Ph.D. Student

ISSN: 2005-307X (Print), 2092-6219 (Online)

before their implementation in software based on the finite element method or difference finite method, which is used to assess geotechnical structures.

This study focuses on defining the parameters of the NorSand constitutive law to model the critical state behaviour of natural sandy soil using the element testing technique. Specifically, the study explores the behaviour of TP-Lisbon sand —an alluvial sand from the Tagus River in the city centre of Lisbon. The constitutive parameters of TP-Lisbon sand were obtained through a comprehensive experimental program. The element testing simulations of NorSand utilised two algorithms: one performed in Visual Basic (VB) by Jefferies *et al.* (2015) and the other by the CONSTRUCT-GEO research group using Fast Lagrangian Analysis of Continua (FLAC) (Itasca 2019). Slight differences between the two algorithms were observed. The results indicate that the NorSand constitutive law effectively describes the behaviour of TP-Lisbon sand in drained triaxial testing conditions by replicating the stress-strain response and volumetric variation during shearing for both contractive and dilative sands. The main contribution of this paper is the validation of soil behaviour characterisation by combing accurate experimental tests and numerical modelling using NorSand constitutive law.

2. NorSand constitutive law

The constitutive model adopted in this study is NorSand (Jefferies 1993). This model was originally proposed for simulating the soil response during triaxial compression by incorporating the concepts of the CSSM framework. This model is applicable to any soil in which particle-to-particle interaction is controlled by contact forces and slips rather than bonds (Jefferies 1993). NorSand includes an idealised work dissipation mechanism, which applies the following three key aspects: (*i*) the yield surface concept of Cam-Clay model; (*ii*) the 'flow-rule' to account for the relative plastic strain increments; and (*iii*) the hardening law, which controls how the yield surface responds to plastic strain.

NorSand constitutive law has been widely implemented to represent the behaviour of several types of granular geomaterials, including sandy soils (Ghafghazi and Shuttle 2008, Jefferies *et al*. 2015) and silty tailings (Shuttle and Cunning 2007, Shuttle and Jefferies 2016). This constitutive law allows for the modelling of soil behaviour under different conditions of axial and radial effective stresses (σ'_a and σ'_r respectively). Such stress combinations can be represented by the mean effective stress $p' = (\sigma_a + 2\sigma_r)/3$ and the deviatoric stress, $q = \sigma_a - \sigma_r$. Nevertheless, the main advantage of NorSand is the representation of soil response at large strains, considering the effects of void ratio and confining pressure through the application of the state parameter, ψ, which relates the difference between the current void ratio e with the void ratio in the critical state e_{cs} (Been and Jefferies, 1985), that is, $\psi = e - e_{cs}$.

NorSand captures a wide range of soil behaviour from very loose to very dense conditions, reproducing the full range of soil behaviour from static liquefaction to dilation of granular soils. This is due to the work-hardening plasticity model derived from the two axioms of critical state theory (Jefferies and Been 2015): (*I*) there is a unique critical state locus for each soil; and (*II*) soils move towards its critical state locus with shear strain, achieving a condition of constant volume and constant mean effective stress.

The yield surface of NorSand has a familiar bullet-like shape, following the same concept introduced by the original Cam-Clay model. The yield surface size is related to the development of particle contacts. Nevertheless, it introduces an important difference: there is an internal cap to avoid that the soil does not unload until low mean effective stress without experimenting yield. This internal cap is taken as a flat plane and its location depends on the current state parameter of the soil (Jefferies *et al*. 2015). Fig. 1 illustrates the NorSand yield surface for two cases: a very loose soil and a very dense soil. Besides, Fig. 1 displays the location of the internal cap, which controls the limiting stress ratio (η_L) that the soil can sustain. Such a parameter is sometimes called the 'Hvorslev Surface', corresponding to the locus of hardening limits for a properly derived yield surface.

The plastic dilatancy (D^P) of NorSand is determined from the idealised stress-dilatancy relation that underlies the model. The intermediate principal strain rate is interpolated from the evolution of the relationship of the development of the stress ratio ($\eta = q/p'$) with the ratio between the volumetric strain increment and deviatoric strain increment ($\delta\varepsilon_v/\delta\varepsilon_s$). This interpolation approach is somewhat unusual for plasticity models, but it is applied to ensure consistency with the work dissipation postulate, which is the basis of the model. The stress-dilatancy behaviour can be interpreted using the CSSM framework by combining the D^P with ψ.

This novel interpretation allows estimating the rate of dilation through the dilatancy rate scaling parameter (χ), which is the linear slope obtained by estimating the maximum dilation rate (d_m) and their corresponding minimum state parameter (ψ_{min}) (Giretti *et al.* 2018). Moreover, the volumetric coupling parameter (N) and the plastic hardening modulus (H) are associated with strength at peak dilatancy (η_{max}) to represent the volumetric coupling and the plastic hardening modulus (Nova 1982). H depends, in principle, on the soil fabric and can often be a function of ψ. The hardening law of NorSand describes how the yield surface increases or decreases in size with plastic straining. The size of the yield surface is controlled by the image stress (p'_i), which forms the object of the hardening law. Such a parameter is called the image stress because it represents a situation in which the critical state is achieved (i.e., zero volume change). This remark can also be observed in Fig. 1.

NorSand has an isotropic hardening rule, which expands or contracts the yield surface, as required by the hardening law, while retaining its shape. The position of the internal cap evolves with the changing state parameter. Whether the yield surface hardens or softens depends on two things: (*i*) the current state parameter and (*ii*) the direction of loading.

The soil properties used in NorSand are familiar and can be estimated by laboratory testing with some flexibility

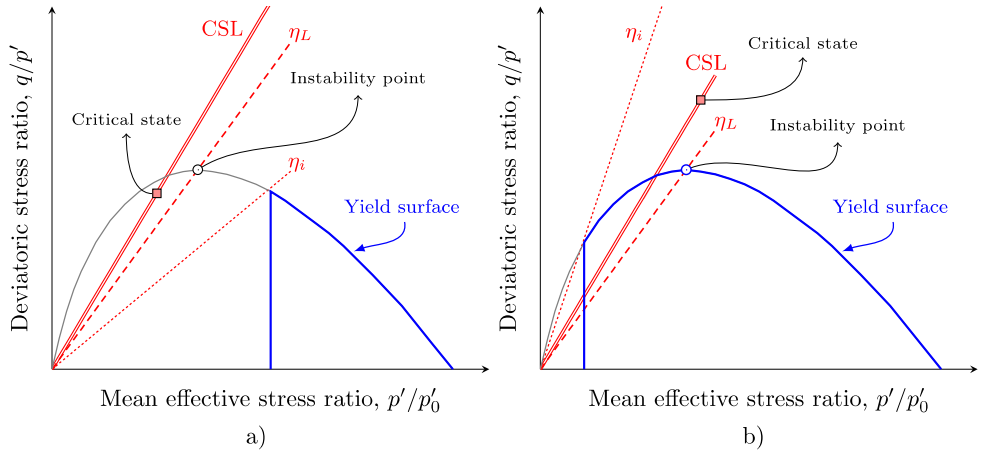

Fig. 1 Illustration of NorSand yield surfaces and limiting stress ratios (after Jefferies *et al*. 2015): (a) very loose sand and (b) very dense sand

Table 1 Parameters for NorSand modelling (after Jefferies and Been 2015)

Internal model parameters	$\psi_i = \psi - \ln\left(\frac{p'_i}{p'}\right)$ where: $\psi = e_0 - e_{cs}$ $M_i = M\left(1 - \frac{N^*\chi\lvert\psi_i\rvert}{M}\right)$
Critical state	$e_{cs} = \Gamma - \lambda(p')$ $\eta_{cs} = M$
Yield surface	$\eta_{\max} = \frac{q_{\max}}{p'_{\max}}$ $\frac{\eta}{M} = 1 - \ln\left(\frac{p'_i}{p'}\right)$ with: $\left(\frac{p'_{max}}{p'}\right) = exp\left(-\frac{\chi\psi_i}{M}\right)$
Hardening rule	On the yield surface: $\frac{\dot{p}'}{p'_i} = H\left(\frac{\eta}{M}\right)\left(\frac{p'}{p'_i}\right)^2\left[exp\left(-\frac{\chi\psi_i}{M}\right) - \frac{p'}{p'_i}\right]\dot{\varepsilon}_q^p$ On the internal surface: $\frac{\dot{p}'}{p'_i} = -\frac{H}{2}\frac{\eta}{M}\lvert\dot{\varepsilon}_q^p\rvert$
Stress-dilatancy	$d_m = M - \eta$ $D_m^p = D^p\left(\frac{M}{\eta}\right)$
Elasticity	$I_r = \frac{G}{p'_0}$ $K = G\frac{2(1+\upsilon)}{3(1-2\upsilon)}$

depending on the level of detail. Hence, all properties are dimensionless and measured through triaxial compression tests. Triaxial testing allows assessing the shear-confinement-volume parameters at critical state condition or 'Critical State Locus' (CSL) in the three-dimensional space $e{:}\,p'{:}\,q$.

This three-dimensional space leads to two projections in two-dimension plans, which depend on the mean effective stress, $p' = (\sigma_a + 2\sigma_r)/3$, the shear or deviatoric stress, $q = \sigma_a - \sigma_r$, and the void ratio of the soil e. The projection of the critical state in the $p'{:}\,q$ space corresponds to a straight line related to the effective critical state friction angle (ϕ'_{cs}), and defines the critical stress ratio, M. The projection of the critical state in the $e{:}\,p'$ space indicates the points where the mean effective stress and void ratio (or volume) are constant. The union of such points represents the CSL, which is plotted using a semi-logarithmic trend, defining the slope λ and the intercept Γ parameters of the CSL. Table 1 summarises the equations for computing NorSand parameters.

In this study, the NorSand constitutive law was selected due to its applicability to granular materials and its theoretical features based on the CSSM framework, which enables modelling the soil response in a wide range of strains. Moreover, NorSand was preferred over other models Besides, NorSand was selected over other models (e.g., SANISAND, PDMY02, PDMY03 or PM4sand) due to its indexing with the ψ, which is not explicitly included in diverse constitutive models. This indexing allows assessing the mechanical response at large strains of granular soils with both contractive and dilative behaviour. Therefore, the element test modelling using NorSand covers both the maximum shear strength and the critical state.

3. Materials and experimental methods

3.1 TP-Lisbon sand

TP-Lisbon sand is an alluvial granular soil with origin in the late Quaternary, which has sedimented next to the Tagus River in the historical centre of Lisbon, in Praça do Comércio site (in Portuguese commonly named 'Terreiro do Paço', TP, that in English means courtyard palace). The constructions surrounding this relevant historical spot of Portugal correspond to old heritage Pombalino masonry buildings. The lithological profile below Terreiro do Paço consists of soil layers composed of fine clean sands and sandy silts with intercalations of plastic soils, which rest over stiff clays deposited in the Miocene (Gouveia *et al.* 2018). The presence of such intercalations seems to indicate

Table 2 Physical properties of TP-Lisbon sand

Parameter	Value
Gs	2.66
e_{max}	1.01
e_{min}	0.64
D_{50}	0.21
FC (%)	2.21
Cc	1.13
Cu	1.69

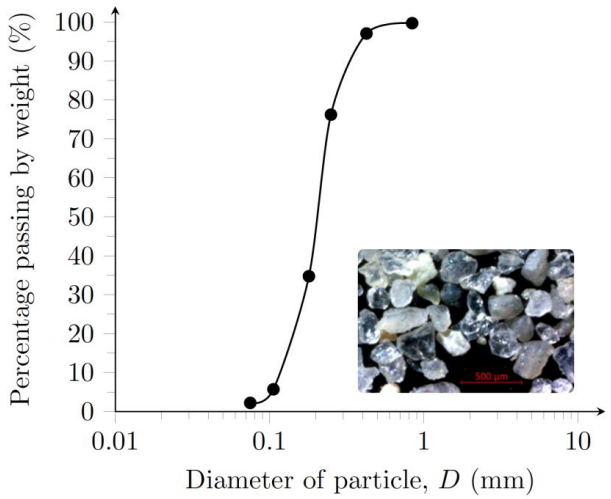

Fig. 2 Particle size distribution of TP-Lisbon sand

that the valley was infilled in a heterogeneous process, corresponding to tidal variations in the Tagus River (Miranda *et al.* 2020, Viana da Fonseca *et al*. 2023). Within the scope of geotechnical exploration for the construction of the Lisbon blue line tunnel of 'Metropolitano de Lisboa', integral samples of TP-Lisbon sand were collected between 13 to 23 m depth. These samples were obtained using a rotary probe attached to a Shelby sampler device able to retrieve integral samples of 110 mm diameter in a site investigation located into the Terreiro do Paço area at the coordinates 38º42'26.6"N–9º8'13.4"W.

Table 2 presents the physical properties of TP-Lisbon measured in the laboratory, namely the specific gravity of solid particles (G_s), the maximum void ratio (e_{max}) and the minimum void ratio (e_{min}). Besides, Table 2 presents the parameters of the grain size distribution; that is, mean diameter (D_{50}), fines content (FC), coefficient of curvature (Cc) and coefficient of uniformity (Cu). Fig. 2 shows the particle size distribution of TP-Lisbon sand. According to the unified soil classification system (USCS), TP-Lisbon sand is classified as poorly graded (SP), with low values of Cu and Cc, which denoted a uniform grain size distribution of the studied soil.

A comprehensive analysis of particle morphology, using Morphologi G3-ID equipment, revealed that TP-Lisbon sand is mainly composed by subangular particles with convexity Cx = 0.96, circularity Ci = 0.88, sphericity S = 0.73, roundness R = 0.38 and regularity ρ = 0.55 (Molina-Gómez and Viana da Fonseca 2021). On the other hand, the mineralogy of TP-Lisbon sand comprises 78% quartz, 8% muscovite, 8% orthoclase and 6% albite (Molina-Gómez *et al*. 2020).

3.2 Testing procedures

A comprehensive experimental programme at the Geotechnical Laboratory of FEUP (LabGEO, University of Porto, Portugal) was carried out to characterise the NorSand parameters of TP-Lisbon sand. Such an experimental programme included a series of advanced monotonic triaxial tests in cells equipped with lubricated end platens and an embedded connection piston into the top-cap or with piezoelectric transducers for bender element (BE) tests.

The use of lubricated end platens allows reducing the influence of platen restraint on stresses in the soil sample during triaxial testing, which induces uniform radial strains and helps to keep the cylindrical shape of the specimen at large axial strain levels (Jefferies and Been 2015, Molina-Gómez and Viana da Fonseca 2021). The embedded connection piston serves to significantly reduce the 'tilting' of the top cap during all phases of triaxial testing, providing more reliable test results (Reid *et al*. 2021, Viana da Fonseca *et al*. 2021, Viana da Fonseca *et al*. 2022). The BE tests were carried out to estimate the small-strain stiffness of the soil (Viana da Fonseca *et al*. 2009).

All soil specimens were remoulded by the dry pluviation method (Quinteros and Carraro, 2023). This method was adopted since it provides homogeneous soil specimens with a fabric similar to the fabric of alluvial soil deposits (Miranda *et al*. 2020, Molina-Gómez *et al*. 2020). Besides, this method ensures the remoulding of soil specimens with a uniform relative density (Jamil *et al*. 2022). The saturation of soil specimens was carried out according to the procedure suggested by Soares and Viana da Fonseca (2016). This saturation procedure incorporated two phases: (*i*) the gentle percolation of a minimum of two times the volume of voids with CO_2 and de-aired water; and (*ii*) the application of backpressure increments at 50 kPa/h under constant effective stress of 10 kPa until 300 kPa is reached. The soil specimens were only considered fully saturated for Skempton's B-value higher than 0.97. However, for the tests conducted in the triaxial cells equipped with piezoelectric transducers, soil specimens were only considered fully saturated when the B-value criterion was verified and also values of compressional wave velocity near or above 1500 m/s were measured (Santamarina *et al*. 2005).

After saturation, soil specimens were isotropically consolidated at different confining effective stress (p'_0). Besides, all soil specimens were sheared at 0.025 mm/min, ensuring an axial strain velocity that does not generate excess of pore pressure during drained shear. Data reported in the shearing phase was corrected considering the effect of membrane restraint using the method of standard ISO 17892-9:2018. At the end of each test, the soil specimens tested in the triaxial cell with lubricated end platens were subjected to freezing to ensure an accurate measurement of the void ratio of soil at the critical state condition *et al*. 2021, Soares and Viana da Fonseca 2016).

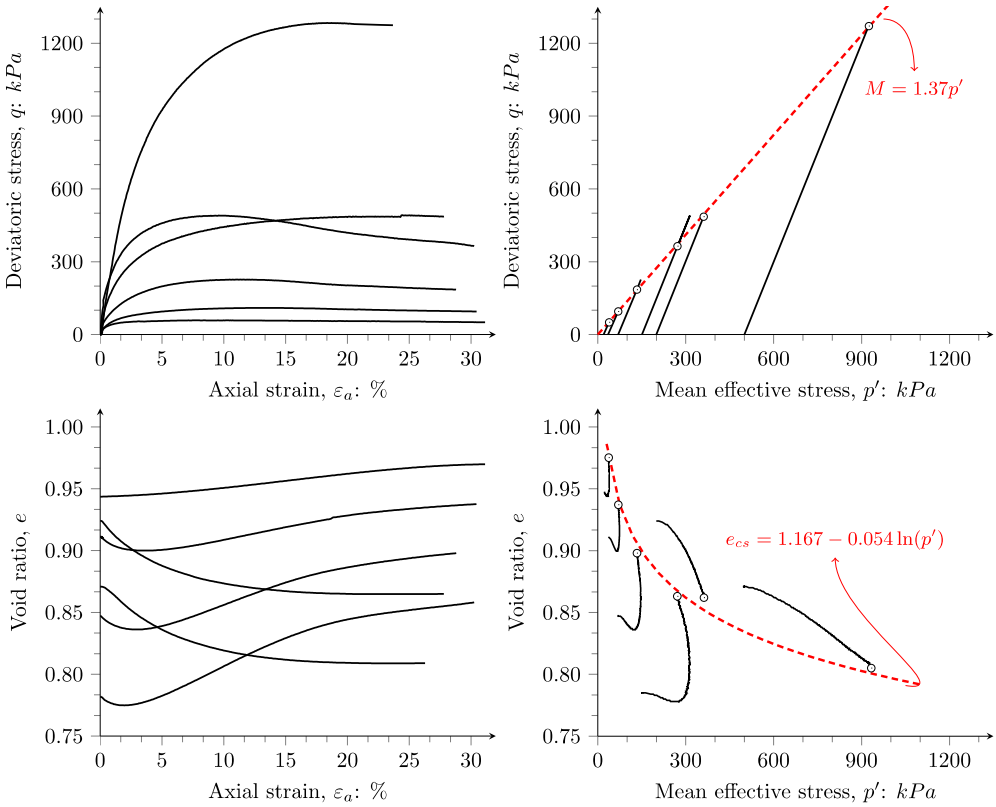

Fig. 3 Results and stress-path of the triaxial tests

On the other hand, bender element (BE) tests were conducted in a triaxial cell equipped with piezoelectric transducers to measure the shear and compression wave velocities (*Vs* and *Vp*), as suggested by Ferreira *et al.* (2021). The procedure of BE testing covers the generation of a single sinusoidal pulse at different frequencies to excite the BE transmitter, including frequency values between 1 to 10 kHz and 25 to 150 kHz to estimate *Vs* and *Vp*, respectively (Molina-Gómez, Viana da Fonseca *et al.* 2023). The time of wave propagation was estimated by applying the first arrival method (Ferreira *et al.* 2021, Lee and Santamarina 2005). The measurement of both *Vs* and *Vp* allows deriving the elastic stiffness properties of TP-Lisbon sand.

The samples tested in the triaxial cells equipped with BE were not freezing to prevent possible damage in these transducers during such a process. However, the final void ratio of for this testing configuration was estimated through the method proposed by Verdugo and Ishihara (1996), which also provides reliable measurements if well implemented (Viana da Fonseca *et al.* 2021).

4. Analysis of results

4.1 Characterising the NorSand parameters for TP-Lisbon sand

Six triaxial tests were conducted at different mean effective stress (p'_0) and relative density (Dr) to characterise the NorSand parameters. These testing conditions ensure the soil testing for different ψ. Two of these tests were performed in soil specimens with contractive behaviour, while four were performed in soil specimens with dilative behaviour. Fig. 3 presents the results and testing paths of the six triaxial tests. From Figure 3, it can be observed that all tests achieved axial strains higher than 25%, indicating that all samples reached the critical state condition. Triaxial test results revealed a unique critical state locus (CSL) for TP-Lisbon sand. Table 3 details the triaxial testing conditions and the values reported at the end of the tests –used to define the critical state locus of TP-Lisbon sand.

According to experimental results, a linear model was adopted to represent CSL of TP-Lisbon sand in both p':q and e:$\log p'$ spaces. In the p':q space, CSL is well represented by a straight line passing through the origin with a strength parameter M = 1.37. In the e:$\log p'$ space, the CSL is well represented by a linear model that follows the form $e_{cs} = \Gamma - \lambda \ln p'$. By applying a linear regression, the values of Γ = 1.167 and λ = 0.054 were derived. CSL parameters were obtained under a correlation coefficient $R^2 > 0.97$. Such a linear approach is suitable for assessing the soil behaviour in the testing conditions (i.e., p' and e ranges) addressed in this study.

A stress-dilatancy analysis for TP-Lisbon sand was carried out based on the triaxial test results that exhibit dilative behaviour. Stress-dilatancy denotes the volumetric changes in granular materials as a result of mobilised shear strains and applied stresses by computing the relation between the volumetric strain increment and the deviatoric strain increment (Been and Jefferies 2004, Xu and Coop

Table 3 Details of triaxial testing

Test name	Triaxial cell	After consolidation		End of test		
		Mean effective stress, p'_0 (kPa)	Relative density, Dr (%)	Deviatoric stress, q_{cs} (kPa)	Mean effective stress, p'_{cs} (kPa)	Void ratio, e_{cs}
Tx-20	LEP	20	18	51	39	0.97
Tx-35	LEP	35	27	95	70	0.94
Tx-70	LEP	70	44	185	134	0.90
Tx-150	LEP	150	62	362	270	0.86
Tx-200	LEP	200	23	487	362	0.87
Tx-500	BE	500	38	923	1279	0.81

Notation: LEP is cell equipped with lubricated end platens; BE is cell equipped with bender elements

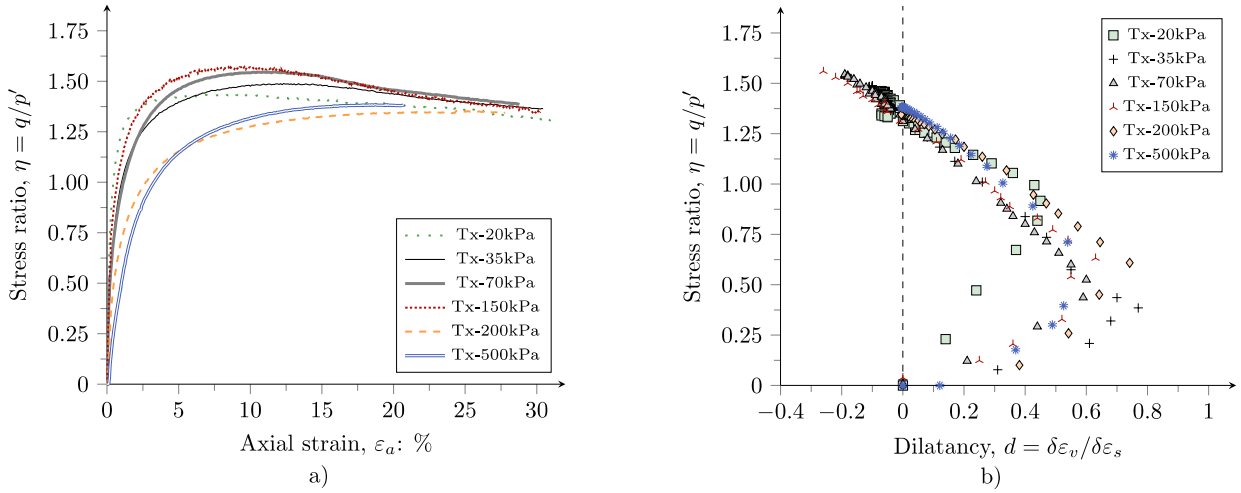

Fig. 4 Stress-dilatancy evolution: (a) stress ratio development and (b) dilation rate

2017). The initial void ratio and contacts between the soil particles control the dilatancy of granular materials (Gong *et al*. 2021). Fig. 5 shows the stress-dilatancy results in terms of the development of the stress ratio ($\eta = q/p'$) and the evolution of mobilised shear strains ($d = \delta\varepsilon_v/\delta\varepsilon_s$). In Fig. 4(a), it can be observed that, after 20% axial strain, η converges to 1.37, which corresponds to the value of M. Moreover, in Fig. 4(b), it can be observed that for $\eta = M = 1.37$, the dilation, d, is zero. This satisfies the second axiom of CSSM –constant volume and stress states of the soil at the critical state condition. The stress-dilatancy parameters were derived to describe the hardening rule of NorSand, which controls the peak strength and plastic strains of the soil during shearing.

It is well known that the maximum dilatancy (d_m) occurs simultaneously at the maximum stress ratio (η_{max}) and the minimum state parameter (ψ_{min}). Nova (1994) stated that the parameters describing the stress-dilatancy behaviour, based on the CSSM framework, are the critical stress ratio (M), the volumetric coupling parameter (N) and the dilatancy rate scaling parameter (χ). Both N and χ parameters can be obtained by assessing the linear relationship between d_m with η_{max} and ψ_m. Fig. 5 presents the results of such a novel interpretation for describing the stress-dilatancy of TP-Lisbon sand. The linear trendline outlined in Fig. 5(a) denotes a parameter N = 0.21 and an intercept value of M = 1.37, where the dilation is zero. Moreover, Fig. 5(b) shows the derivation of χ = 3.73.

Loads within the assembly competence comprise reversible distortions of the soil particles and lie within the yield surface (Shuttle and Jefferies 2016). Therefore, elastic properties allow NorSand to identify the onset of permanent soil deformations. Elastic properties of TP-Lisbon sand were assessed by estimating the stress-dependency of seismic wave velocities, namely shear and compression wave velocities (Vs and Vp). For this purpose, dry and saturated soil specimens were subjected to a series of bender element (BE) tests at different isotropic confinement stresses. The results of Vp for saturated conditions revealed values in about 1500 m/s, confirming that in these conditions, the P-wave propagates predominantly through the water. Fig. 6 shows the stress-dependency of seismic wave velocities of TP-Lisbon sand.

A contrast between Vs results of dry and saturated specimens revealed no substantial effects concerning the degree of saturation on the small-strain stiffness of TP-Lisbon sand. On the other hand, from the BE test results on dry specimens, Poisson's ratio (ν) was estimated for each mean effective stress, p', using the elastic relation between Vs and Vp (see Eq. (1)).

$$\nu = \frac{0.5\left(\frac{Vp}{Vs}\right)^2 - 1}{\left(\frac{Vp}{Vs}\right)^2 - 1} \quad (1)$$

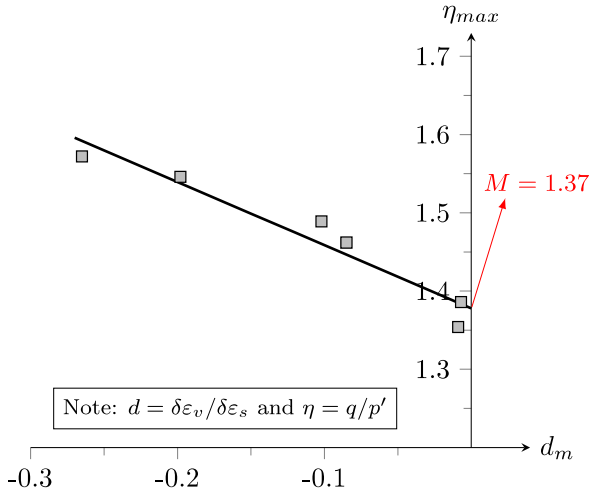

(a)

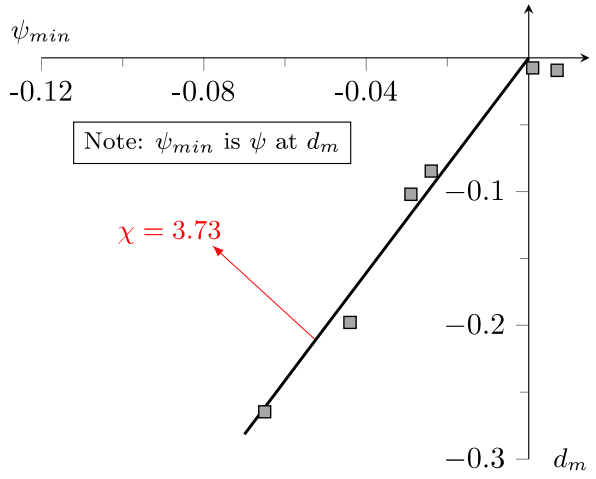

(b)

Fig. 5 Interpretation of stress-dilatancy based on CSSM: (a) dilatancy rate at peak stresses and (b) dilatancy scaling

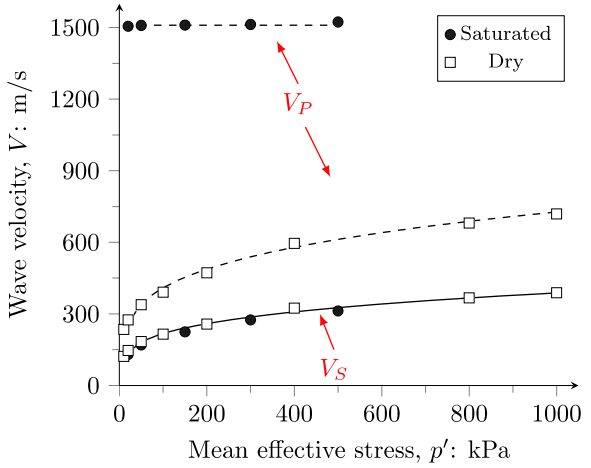

Fig. 6 Stress-dependent of seismic wave velocities

By applying Equation 1 on the data of Fig. 6 and conducting a statistical analysis, a Poisson's ratio ν = 0.29 was established for TP-Lisbon sand. Such value has a variability of about 5%. Poisson's ratio ν = 0.29 agree with results reported for other silica sands from piezoelectric transducers by other authors (Ferreira *et al*. 2021,Suwal and Kuwano 2013, Wichtmann and Triantafyllidis 2010). However, ν may have slight changes due to variations in relative density (Gu *et al.* 2013), which do not significantly affect the results of NorSand simulations (Jefferies and Been, 2015).

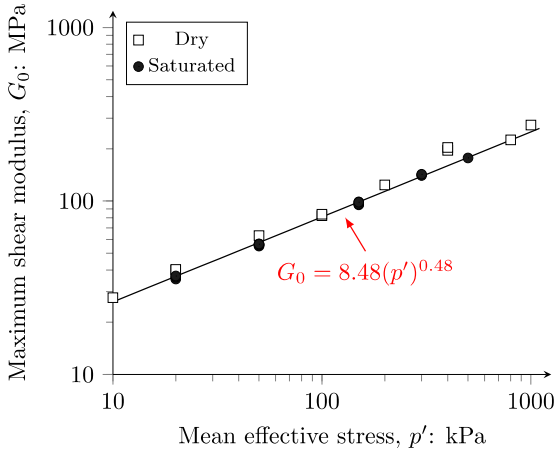

Fig. 7 Stress-dependency of maximum shear modulus

The small-strain stiffness of soils is generally referred to as the maximum shear modulus, G_0. This elastic parameter is computed using the equations of isotropic elasticity; that is, $G_0 = \rho Vs^2$. Like Vs, G_0 is also strongly affected by the stress state of the soil. However, such an effect can be estimated for different stress states using the stress-dependency of seismic wave velocities. Hence, a model for describing the stress-dependency of G_0 for TP-Lisbon sand was derived. The model adopted in this research complies with the forms identified by Molina-Gómez *et al.* (2020). Eq. (2) defines the model for describing the evolution of G_0 as a function of p'.

$$G_0 = A(p')^n \tag{2}$$

where A is a material coefficient that captures the influence of the particle shape, soil fabric or structure, bonding or cementation of the particles, and n is a power exponent that reflects the sensitivity of the shear modulus to the confining pressure.

Fig. 7 presents the model results for describing the evolution of G_0 as a function of p' for both dry and saturated conditions. The results show a good agreement between dry and saturated conditions, confirming no important effects of the degree of saturation on the small-strain stiffness of TP-Lisbon sand.

The soil properties presented up to here are associated with the mechanical behaviour estimated in the laboratory by triaxial testing. However, plastic hardening is different because a property that describes this behaviour has yet to be well identified (Jefferies *et al*. 2015, Shuttle and Jefferies 2016). NorSand adopts a dimensionless hardening modulus (H) to describe the plastic hardening of soils (Jefferies 1993). This parameter relates an initial hardening modulus (H_0) with the state parameter at the beginning of the triaxial

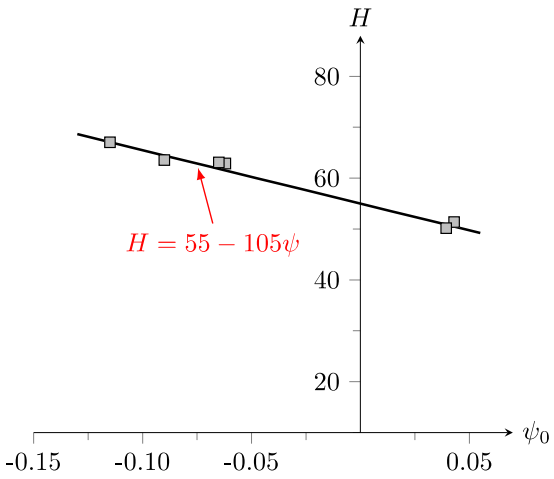

Fig. 8 Fitting of hardening modulus

Table 4 NorSand parameters of TP-Lisbon sand

Framework	Parameter	Value	Typical range*
Critical state	M	1.37	1.2 to 1.5
	λ	0.054	0.03 to 0.15
	Γ	1.16	0.85 to 1.40
Dilatancy	N	0.21	0.2 to 0.5
	χ	3.73	2.5 to 4.5
	H	55-105 ψ	50 to 500
Elasticity	A (MPa)	8.48	3.0 to 13
	n	0.48	0.3 to 0.6
	ν	0.29	0.1 to 0.35

*Data from Cho *et al.* (2006) and Jefferies *et al.* (2015)

shearing (ψ_0), providing a general trend

$$H = H_0 - H_y \psi_0 \quad (3)$$

The constants in Eq. (3) are obtained by a visual comparison between experimental and numerical results (Jefferies and Been 2015), leading to an iterative procedure to find the best fitting that describes the linear relation between H and ψ_0. Fig.8 presents the linear trend of H to describe the plastic hardening of TP-Lisbon sand, with the properties $H_0 = 55$ and $H_y = 105$ under an $R^2 > 0.95$.

Based on the comprehensive laboratory characterisation of TP-Lisbon sand presented herein, the NorSand parameters were defined. Table 4 summarises the NorSand properties of TP-Lisbon sand. These parameters will be adopted for the subsequent numerical simulations of element tests using the NorSand constitutive law.

4.2 Modelling of soil behaviour with NorSand

NorSand has no closed-form solution; thus, the implementation of numerical integration is required in element tests that involve this constitutive law (Jefferies and Been 2015). The modelling of soil behaviour using NorSand is available in a downloadable supplemental spreadsheet provided by Jefferies *et al.* (2015). Such a spreadsheet works on a Visual Basic (VB) code with the Euler integration method, which is a simple method with a small step size, adequate when dealing with triaxial test data. Moreover, NorSand is included in the constitutive models of Fast Lagrangian Analysis of Continua (FLAC) (Itasca 2019), which is ideal for numerical modelling of advanced geotechnical analyses that require large strains or displacements. Both FLAC and VB algorithms use the explicit integration method for simulating element tests.

NorSand modelling was conducted herein using the complete set of properties referred to in Table 4 and two algorithms developed in VB and FLAC. In addition, the numerical simulations were carried out considering the same conditions of the triaxial tests indicated in Table 3; that is, the initial state parameter (ψ_0) for both relative density and mean effective stress (p'_0) after consolidation. NorSand results were validated by comparing the entire stress-strain behaviour obtained by numerical element testing results of VB and FLAC against the experimental data obtained in the laboratory.

Fig. 9 shows the typical results of the numerical modelling of NorSand using VB and FLAC for two contractive and two dilative tests. Besides, these figures present a comparison between numerical results with their corresponding laboratory data. From Fig. 9, it can be observed that NorSand simulated well the drained triaxial tests of TP-Lisbon sand. In addition, the results of VB and FLAC codes have similar tendencies and fit well with the laboratory data, showing slight differences between the results of both FLAC and VB simulations. Although NorSand can replicate both contractive and dilative behaviours, results revealed the best fitting for the stress-strain and volumetric variation curves (i.e., ε_a vs q and ε_a vs ε_v) in the dilative tests.

Table 5 summarises the results at the critical state of the NorSand numerical modelling simulations. Besides, it compares these results against laboratory data for each test. Results in Table 5 showed similar values between laboratory data with NorSand simulations in terms of mean effective stress at the critical state (p'_{cs}) and shear strength at the critical state (q_{cs}), and void ratios at the critical state (e_{cs}) for all tests. Fig. 10 presents test paths of numerical simulations and the points used to define the critical state condition of TP-Lisbon sand. From Fig. 10, it can be observed that NorSand constitutive law computation accurately predicts critical state behaviour in both contractive and dilative sands using FLAC and VB codes. Moreover, the test paths obtained using NorSand element testing follow the same tendency of experimental results reported in Fig. 3, and these tendencies do not differ from FLAC and VB algorithms, confirming the accuracy of NorSand constitutive law.

5. Conclusions

This paper has presented the results of a detailed characterisation of the geomechanical properties of TP-Lisbon sand for the calibration and application of NorSand constitutive law. This sand is an alluvial soil from the city

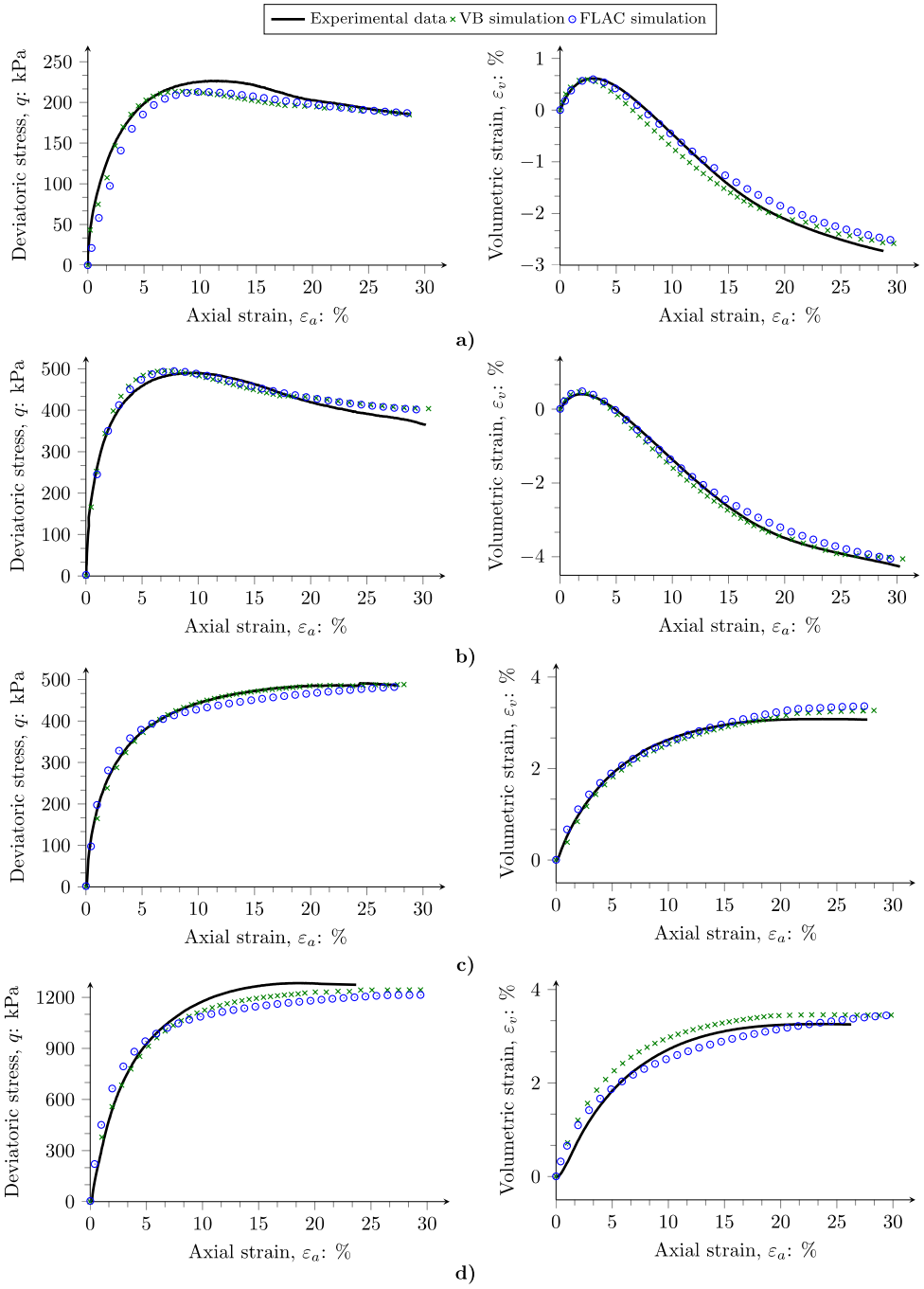

Fig. 9 Results of NorSand simulations compared against laboratory tests: (a) Tx-70, (b) Tx-150, (c) Tx-200 and (d) Tx-500

of Lisbon next to the Tagus River. The behaviour of TP-Lisbon sand was simulated using two codes developed in VB and FLAC, which integrate the NorSand formulation.

From experimental and numerical results, the following main conclusions can be drawn:

• A characterisation focused on critical state locus, stress-dilatancy and elasticity on TP-Lisbon sand was carried out by advanced triaxial testing, which is not common in numerous geotechnical laboratories worldwide. From this characterisation, the NorSand constitutive law was calibrated. NorSand parameters of TP-Lisbon sand are within the typical ranges for sands reported in the literature.

• NorSand modelling revealed that this constitutive law describes well the behaviour of TP-Lisbon sand under drained conditions. Results of numerical simulations showed a good agreement with the experimental data for both contractive and dilative tests. The best fitting of ε_a vs q and ε_a vs ε_v was observed for the simulation of dilative tests

• Simulations of VB and FLAC codes also showed similar values of the experimental data at critical state conditions in the p':q and e:log p' spaces. NorSand results revealed very similar test paths to the experimental data, which defined the critical state locus, validating the good prediction of contractive and dilative behaviour of TP-Lisbon sand by

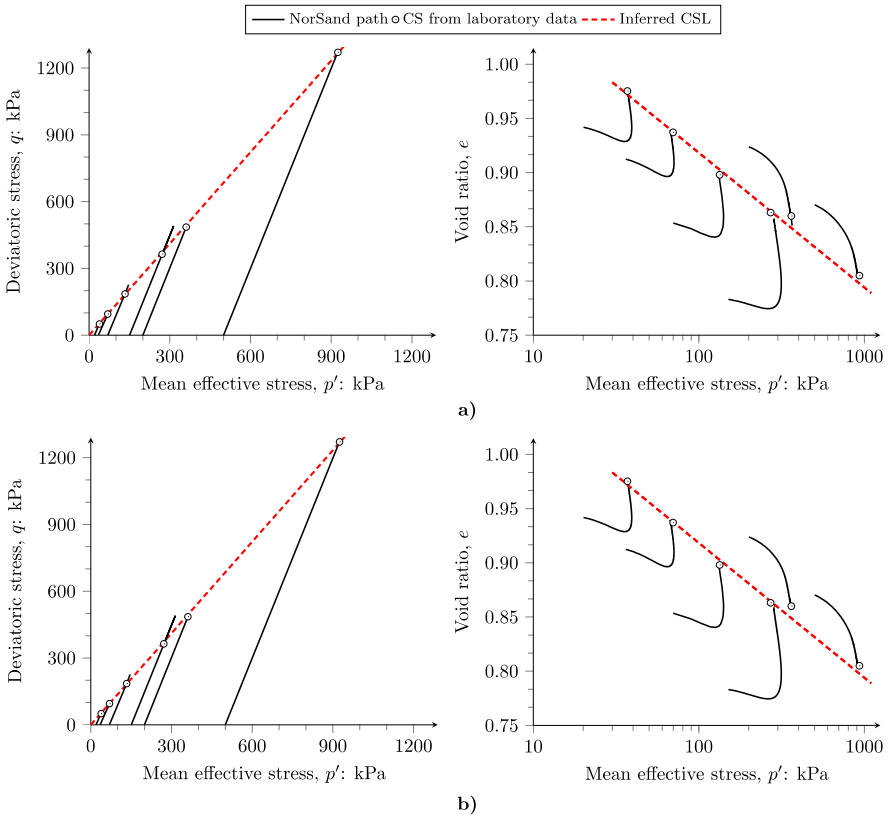

Fig. 10 CSL of element testing by NorSand modelling: (a) FLAC test paths and (b) VB test paths

Table 5 Summary of results at critical state of triaxial tests and numerical element testing

Test name	ψ_0	Lab data			VB			FLAC		
		p'_{cs} (kPa)	q_{cs} (kPa)	e_{cs}	p'_{cs} (kPa)	q_{cs} (kPa)	e_{cs}	p'_{cs} (kPa)	q_{cs} (kPa)	e_{cs}
Tx-20	-0.07	51	39	0.97	53	37	0.97	52	37	0.97
Tx-35	-0.06	95	70	0.94	97	68	0.93	94	68	0.94
Tx-70	-0.09	195	134	0.90	195	135	0.90	194	135	0.89
Tx-150	-0.12	362	270	0.86	434	285	0.86	400	283	0.86
Tx-200	0.04	362	487	0.87	361	487	0.87	361	482	0.88
Tx-500	0.03	924	1273	0.81	918	1254	0.81	918	1234	0.81

this constitutive law.

• A agreement was obtained between experimental data and numerical simulations. This can be attributed mainly to the adequacy of the testing programme and the quality of laboratory procedures and analyses to obtain the NorSand parameters, which have been purposely detailed in this work. Therefore, based on the good agreement between experimental and numerical results, further research can be conducted to assess the performance of geotechnical structures using NorSand.

Acknowledgments

This work was financially supported by UIDB/04708/2020 and UIDP/04708/2020 of CONSTRUCT – Institute of R&D in Structures and Construction, Portugal funded by the national funds through the FCT/MCTES (PIDDAC). The second and fourth authors acknowledge the Portuguese Foundation for Science and Technology (FCT) for the support of the grants SFRH/BD/146265/2019 and SFRH/BD/143817/2019, respectively. Acknowledgements are especially due to Dr Cristina Raminhos from 'Metropolitano de Lisboa, E.P.E.' for providing the samples of TP-Lisbon sand. The authors also acknowledge the technical support given by Eng. Daniela Coelho and Mr. Armando Pinto of LabGeo during the development of the experimental program.

References

Been, K. and Jefferies, M. (1985), "A state parameter for sands", *Géotechnique*, **35**(2), 99-112.

https://doi.org/10.1680/geot.1985.35.2.99.

Been, K. and Jefferies, M. (2004), "Stress-dilatancy in very loose sand", *Can. Geotech. J.*, **41**(5), 972-989. https://doi.org/10.1139/T04-038.

Boulanger, R.W. and Ziotopoulou, K. (2017), *PM4SAND (version 3.1): A sand plasticity model for earthquake engineering applications*. Davis, California, USA. Retrieved from https://ucdavis.app.box.com/s/wvyr69j5cmq3iu6o9fpzlmzif8r2bwv8.

CEN. ISO 17892-9 (2018), Geotechnical investigation and testing - Laboratory testing of soil - Part 9, Consolidated triaxial compression tests on water saturated soils, International Organization for Standardization, Brussels.

Cho, G.C., Dodds, J. and Santamarina, J.C. (2006), "Particle shape effects on packing density, stiffness, and strength: Natural and crushed sands", *J. Geotech. Geoenviron. Eng.*, **132**(5), 591-602. https://doi.org/10.1061/(ASCE)1090-0241(2006)132:5(591).

Desai, C.S. (2005), "Constitutive modeling for geologic materials: significance and directions", *Int. J. Geomech.*, **5**(2), 81-84. https://doi.org/10.1061/(ASCE)1532-3641(2005)5:2(81).

Ferreira, C., Díaz-Durán, F., Viana da Fonseca, A. and Cascante, G. (2021), "New approach to concurrent Vs and Vp measurements using bender elements", *Geotech. Test. J.*, **44**(6), 1801. https://doi.org/10.1520/GTJ20200207.

Ghafghazi, M. and Shuttle, D. (2008), "Interpretation of sand state from cone penetration resistance", *Géotechnique*, **58**(8), 623-634. https://doi.org/10.1680/geot.2008.58.8.623.

Giretti, D., Fioravante, V., Been, K. and Dickenson, S. (2018), "Mechanical properties of a carbonate sand from a dredged hydraulic fill", *Géotechnique*, **68**(5), 410-420. https://doi.org/10.1680/jgeot.16.P.304.

Gong, J., Cheng, L., Zhao, L., Zou, J., Li, L. and Nie, Z. (2021), "Study on the packing and shear characteristics of granular mixtures via the DEM", *Geomech. Eng.*, **27**(3), 223-237. https://doi.org/10.12989/gae.2021.27.3.223.

Gouveia, F., Viana da Fonseca, A., Carrilho Gomes, R. and Teves-Costa, P. (2018), "Deeper Vs profile constraining the dispersion curve with the ellipticity curve: A case study in Lower Tagus Valley, Portugal", *Soil Dyn. Earthq. Eng.*, 109, 188-198. https://doi.org/10.1016/J.SOILDYN.2018.03.010.

Gu, X., Yang, J. and Huang, M. (2013), "Laboratory measurements of small strain properties of dry sands by bender element", *Soils Found.*, **53**(5), 735-745. https://doi.org/10.1016/j.sandf.2013.08.011.

Jamil, I., Ahmad, I., Ullah, W., Junaid, M. and Khan, S.A. (2022), "Uniform large scale cohesionless soil sample preparation using mobile pluviator", *Geomech. Eng.*, **28**(5), 521-529. https://doi.org/10.12989/gae.2022.28.5.521.

Jefferies, M. (1993), "Nor-Sand: a simple critical state model for sand", *Géotechnique*, **43**(1), 91-103. https://doi.org/10.1680/geot.1993.43.1.91.

Jefferies, M. and Been, K. (2015), *Soil Liquefaction: A Critical State Approach* (2nd ed.). Milton Park, Abingdon: CRC Press.

Jefferies, M., Shuttle, D. and Been, K. (2015), "Principal stress rotation as cause of cyclic mobility", *Geotech. Res.*, **2**(2), 66-96. https://doi.org/10.1680/jgere.15.00002.

Lee, J.S. and Santamarina, J.C. (2005), "Bender elements: performance and signal interpretation", *J. Geotech. Geoenviron. Eng.*, **131**(9), 1063-1070. https://doi.org/10.1061/(ASCE)1090-0241(2005)131:9(1063).

Mendoza, C. and Muniz de Farias, M. (2020), "Critical state model for structured soil", *J. Rock Mech. Geotech. Eng.*, **12**(3), 630–641. https://doi.org/10.1016/j.jrmge.2019.12.006.

Miranda, L., Caldeira, L., Serra, J. and Gomes, R.C. (2020), "Dynamic behaviour of Tagus River sand including liquefaction", *Bull. Earthq. Eng.*, **18**(10), 4581-4604. https://doi.org/10.1007/s10518-020-00881-5.

Molina-Gómez, F., Caicedo, B. and Viana da Fonseca, A. (2019), "Physical modelling of soil liquefaction in a novel micro shaking table", *Geomech. Eng.*, **19**(3), 229-240. https://doi.org/10.12989/gae.2019.19.3.229.

Molina-Gómez, F. and Viana da Fonseca, A. (2021), "Key geomechanical properties of the historically liquefiable TP-Lisbon sand", *Soils Found.*, **61**(3), 836-856. https://doi.org/10.1016/j.sandf.2021.03.004.

Molina-Gómez, F., Viana da Fonseca, A., Ferreira, C. and Caicedo, B. (2023), "Improvement of cyclic liquefaction resistance induced by partial saturation: An interpretation using wave-based approaches", *Soil Dyn. Earthq. Eng.*, **167**, 107819. https://doi.org/10.1016/j.soildyn.2023.107819.

Molina-Gómez, F., Viana da Fonseca, A., Ferreira, C. and Camacho-Tauta, J. (2020), "Dynamic properties of two historically liquefiable sands in the Lisbon area", *Soil Dyn. Earthq. Eng.*, **132**, 106101. https://doi.org/10.1016/j.soildyn.2020.106101.

Nieto-Leal, A. and Kaliakin, V.N. (2021), "Additional insight into generalized bounding surface model for saturated cohesive soils", *Int. J. Geomech.*, **21**(6). https://doi.org/10.1061/(ASCE)GM.1943-5622.0002012.

Nova, R. (1982), "A constitutive model for soil under monotonic and cyclic loading", (Eds., G. Pande and O. Zienkiewicz), *Soil Mechanics – Transient and Cyclic Loads*, 343-373. Chichester, UK: Wiley.

Nova, R. (1994), "Controllability of the incremental response of soil specimens subjected to arbitrary loading programmes", *J. Mech. Behavior Mater.*, 5(2), 193-201. https://doi.org/10.1515/JMBM.1994.5.2.193.

Petalas, A.L., Dafalias, Y.F. and Papadimitriou, A.G. (2020), "SANISAND-F: Sand constitutive model with evolving fabric anisotropy", *Int. J. Solids Struct.*, **188-189**, 12-31. https://doi.org/10.1016/j.ijsolstr.2019.09.005.

Quinteros, V.S. and Carraro, J. A. H. (2023), "The initial fabric of undisturbed and reconstituted fluvial sand", *Géotechnique*, **73**(1), 1-15. https://doi.org/10.1680/jgeot.20.P.121.

Ramos, C., Viana da Fonseca, A. and Vaunat, J. (2015), "Modeling flow instability of an Algerian sand with the dilatancy rule in CASM", *Geomech. Eng.*, **9**(6), 729-742. https://doi.org/10.12989/gae.2015.9.6.729.

Reid, D., Fourie, A., Ayala, J.L., Dickinson, S., Ochoa-Cornejo, F., Fanni, R. and Suazo, G. (2021). "Results of a critical state line testing round robin programme", *Géotechnique*, **71**(7), 616-630. https://doi.org/10.1680/jgeot.19.p.373.

Santamarina, J.C., Rinaldi, V.A., Fratta, D., Klein, K.A., Wang, Y.-H., Cho, G.C. and Cascante, G. (2005), "A survey of elastic and electromagnetic properties of near-surface soils", (Ed., D.K. Butler), *Near-Surface Geophysics*, 71-87. Society of Exploration Geophysicists. https://doi.org/10.1190/1.9781560801719.ch4

Schofield, A.N. and Wroth, C.P. (1968), *Critical State Soil Mechanics*, **25**, https://doi.org/10.1111/j.1475-2743.1987.tb00718.x.

Shuttle, D. and Cunning, J. (2007), "Liquefaction potential of silts from CPTu", *Can. Geotech. J.*, **44**(1), 1-19. https://doi.org/10.1139/T06-086.

Shuttle, D. and Jefferies, M. (2016), "Determining silt state from CPTu", *Geotech. Res.*, **3**(3), 90-118. https://doi.org/10.1680/jgere.16.00008.

Soares, M. and Viana da Fonseca, A. (2016), "Factors affecting steady state locus in triaxial tests", *Geotech. Test. J.*, **39**(6), 20150228. https://doi.org/10.1520/GTJ20150228.

Suwal, L.P. and Kuwano, R. (2013), "Statically and dynamically measured poisson's ratio of granular soils on triaxial laboratory specimens", *Geotech. Test. J.*, **36**(4), 20120108. https://doi.org/10.1520/GTJ20120108.

Taiebat, M., Dafalias, Y.F., Taiebat, M. and Dafalias, Y.F. (2008), "SANISAND: Simple anisotropic sand plasticity model", *Int. J. Numer. Anal. Method. Geomech.*, **32**(8), 915-948. https://doi.org/10.1002/NAG.651.

Verdugo, R. and Ishihara, K. (1996), "The steady state of sandy soils", *Soils Found.*, **36**(2), 81-91. https://doi.org/10.3208/sandf.36.2_81.

Viana da Fonseca, A., Cordeiro, D. and Molina-Gómez, F. (2021), "Recommended procedures to assess critical state locus from triaxial tests in cohesionless remoulded samples", *Geotechnics*, **1**(1), 95-127. https://doi.org/10.3390/GEOTECHNICS1010006.

Viana da Fonseca, A., Cordeiro, D., Molina-Gómez, F., Besenzon, D., Fonseca, A. and Ferreira, C. (2022), "The mechanics of iron tailings from laboratory tests on reconstituted samples collected in post-mortem Dam I in Brumadinho", *Soils Rocks*, **45**(2), 1-20. https://doi.org/10.28927/SR.2022.001122.

Viana da Fonseca, A., Ferreira, C. and Fahey, M. (2009), "A framework interpreting bender element tests, combining time-domain and frequency-domain methods", *Geotech. Test. J.*, **32**(2), 100974. https://doi.org/10.1520/GTJ100974.

Viana da Fonseca, A., Molina-Gómez, F. and Ferreira, C. (2023), "Liquefaction resistance of TP-Lisbon sand: a critical state interpretation using in situ and laboratory testing", *Bull. Earthq. Eng.*, **21**(2), 767-790. https://doi.org/10.1007/s10518-022-01577-8.

Wichtmann, T., Fuentes, W. and Triantafyllidis, T. (2019), "Inspection of three sophisticated constitutive models based on monotonic and cyclic tests on fine sand: Hypoplasticity vs. Sanisand vs. ISA", *Soil Dyn. Earthq. Eng.*, **124**, 172-183. https://doi.org/10.1016/j.soildyn.2019.05.001.

Wichtmann, T. and Triantafyllidis, T. (2010), "On the influence of the grain size distribution curve on P-wave velocity, constrained elastic modulus Mmax and Poisson's ratio of quartz sands", *Soil Dyn. Earthq. Eng.*, **30**(8), 757-766. https://doi.org/10.1016/j.soildyn.2010.03.006.

Wood, D.M. (2004), *Geotechnical Modelling* (1st Ed.), Milton Park, Abingdon: CRC Press.

Xu, L. and Coop, M.R. (2017). "The mechanics of a saturated silty loess with a transitional mode", *Géotechnique*, **67**(7), 581-596. https://doi.org/10.1680/jgeot.16.P.128.

Yang, Z., Elgamal, A. and Parra, E. (2003), "Computational model for cyclic mobility and associated shear deformation", *J. Geotech. Geoenviron. Eng.*, **129**(12), 1119-1127. https://doi.org/10.1061/(ASCE)1090-0241(2003)129:12(1119).